*Biochimica et Biophysica Acta*, 1020 (1990) 57–64
Elsevier



BBABIO 43283

# Kinetic optimization of bacteriorhodopsin by aspartic acid 96 as an internal proton donor

A. Miller [1] and D. Oesterhelt [2]

[1] *Consortium für elektrochemische Industrie, München and* [2]*Max-Planck-Institut für Biochemie, Martinsried (F.R.G.)*

(Received 30 January 1990)
(Revised manuscript received 5 July 1990)

Key words: Bacteriorhodopsin; Schiff base; Enzyme kinetics; pH; Proton donor

**The reprotonation of the Schiff base in bacteriorhodopsin (M-decay) was measured in water and deuterium oxide as a function of pH (pD) and ionic strength. Comparison of the wild-type and two mutated proteins (D96 → N or G) clearly demonstrated the function of aspartic acid 96 as an internal protein proton donor for this reaction. Its removal lowers the Arrhenius activation energy of the reaction from 75 kJ / mol to 32 kJ / mol (D96 → N) and 18 kJ / mol (D96 → G) at pH 7 and 10 mM ionic strength. Concomitant with this change is a drastic decrease in rate constant from 166 $s^{-1}$ to 0.4 $s^{-1}$ (D96 → N) and 5 $s^{-1}$ (D96 → G) at pH 7 and 20°C. The effect is due to a small decrease in the free energy of activation but due mainly to a large decrease in the entropy of activation of the mutant proteins. This exemplifies clearly the advantage of a spatially fixed proton donor selected by the protein structure. Lack of aspartic acid 96 also renders the proton pump dependent on external pH (physiologically important) and ionic strength (of no physiological importance). The influences of both parameters on the reaction kinetics can be explained if pH-induced surface potential and surface charge changes at the membrane-bulk interface are taken into account.**

## Introduction

Proton transfer reactions in protein structures are common and best known for acid-base catalyzed reactions in enzymology [1,2]. In vectorial reactions of membrane-bound catalysts proton translocation is of equal importance. Lactose permease, protein translocating ATPase and bacteriorhodopsin are selected examples of these catalysts [3–6]. In their protein structures protons have to cross distances in the range of tenths of ångstroms. The structural details of these proton pathways are not known at atomic resolution. A less well studied example of a known structure is presented by the reaction center in purple non-sulfur bacteria, where protons reach the so-called $Q_B$ site by travelling for about 10 A through a hydrogen-bonded network of amino acid side chains [7].

Bacteriorhodopsin (BR) from Halobacteria has the advantage of presenting the structurally most simple case of an active transporter, i.e., a proton pump. Seven transmembrane helices form an intrahelical pore space through which, in all likelihood, the protons are transferred from the cytoplasm of a cell to the medium [8]. The proton translocation in BR is driven by a thermoreversible all-*trans* to 13-*cis* photoisomerization of its retinylidene chromophore which blocks the intrahelical pore for protons, [9]. The simplest, but also most plausible hypothesis for BR's functional mechanism, is that the protonated C=N double bond between retinal and lysine residue 216 of the polypeptide chain acts as an active proton transfer switch. Not only movement of the positively charged nitrogen is a consequence of *trans* to *cis* isomerization but deprotonation of the Schiff base is an absolutely necessary step in the catalytic cycle. The Schiff base which is located near the middle of the membrane [20] releases a proton to the medial side and receives a proton back from the cytoplasmic side. The key intermediate is the so-called M-state, which has a maximum absorption at 412 nm [10]. Its decay is indicated by a red shift in the spectrum due to the formation of a protonated Schiff base. This reaction therefore must involve a reprotonation pathway from the cytoplasmic surface of the protein which is passed by the proton in about 5 ms. This pathway may include many amino-acid side-chains and water molecules, but is kinetically dominated by the protonated aspartic acid side-chain 96, serving directly or indirectly as a spatially fixed proton donor for the Schiff base in the M-state

Correspondence: D. Oesterhelt, Max-Planck-Institut für Biochemie, Am Klopferspitz, D-8033 Martinsried/München, F.R.G.

[11–13]. Removal of this side-chain by genetic techniques slows the proton pump frequency to physiologically inefficient levels as a result of retardation of M-decay in the catalytic cycle. This defect in a point-mutated bacteriorhodopsin Asp → Asn is fully balanced by addition of azide [14].

Such mutant proteins are well suited for studying proton transfer in protein structures under defined conditions. A detailed analysis of the kinetic parameters of this reaction is presented here.

## Materials and Methods

Strains, cell cultures and purple membranes containing mutated bacteriorhodopsin D96 → N or D96 → G were produced as described [15–17]. Purple membranes were used as prepared or transferred into deuterium oxide. For this, all solutions and buffers were prepared in $D_2O$. Purple membranes were resuspended in $D_2O$, illuminated for 30 min with orange light (150 W projector, OG515 Schott) and centrifuged at 50000 rpm for 30 min. This was repeated three times before final resuspension in the appropriate deuterated medium. All buffers were adjusted with a glass-electrode calibrated in $H_2O$-containing buffer. The p*D* values of the deuterated solution were adjusted to a value of about 0.4 above the indicated pH values. The exact relationship for a specific buffer composition and ionic strength condition was obtained from Ref. 18.

M-decay times of mutated bacteriorhodopsins were analyzed in a home built flash photolysis apparatus. White light, filtered through a cut-off filter (OG515, Schott, Jena), was applied as actinic flash with about a 100 μs duration causing absorbance changes in the sample of about 0.05. This corresponded to about 20% bleaching of the initial state of $BR_{570}$. Absorption changes were detected with monochromatic light at 405 nm (half-width 10 nm) and an intensity lower than 3 $\mu W/cm^2$ at M-decay times shorter than 20 $s^{-1}$ and lower than 0.2 $\mu W/cm^2$ for times longer than 20 s. These conditions prevented significant contributions of photochemical back-reactions of the M-state to $BR_{570}$ caused by the measuring light beam. Although the difference spectra in Fig. 1 demonstrate measurable amounts of the N-intermediate in the photostationary state mixture, no deviation from a monophasic decay of M was found under any of the experimental conditions applied, except for very long decay times. These photostationary state mixtures were analyzed and recorded under conditions of constant actinic light sources irradiating the samples with light between 515 and 620 nm (20 $mW/cm^2$). All membrane suspensions were buffered at 10 mM concentrations with citrate at pH/p*D* 4 and 5, with phosphate between pH/p*D* 6 and 8 and with Tris above pH/p*D* 8. Ionic strength below 10 mM was adjusted by a buffer of the appropriate concentration, above 10 mM sodium, magnesium or potassium chloride (Fig. 3) was added. Stock solutions of purple membranes in water or deuterium oxide were diluted to the appropriate conditions at an optical absorbance at 570 nm of about 0.5.

## Results

*Kinetics and activation parameters*

Both mutant bacteriorhodopsins D96 → N and D96 → G are physiologically inactive proton pumps. This effect is caused by their slow catalytic cycles running with a frequency of about 5 (D96 → G) and 0.4 (D96 → N) per second (Table I). The photocycle of these molecules is normal for its initial reactions but the slowed decay of the M-intermediate determines the low overall rate. Fig. 1A shows the absolute spectra of the initial and the M-state as well as the difference spectrum of both forms under photostationary conditions. When the actinic light was turned off the 410 nm absorption of the M species decreased due to the red colour shift upon protonation of the C=N double bond of the

TABLE I

*Activation parameters of the M-decay for BR and the mutant proteins at pH 7 and 10 mM ionic strength*

Values were calculated from the decay times measured between 5 and 35 °C according to Arrhenius:

$$k = f \cdot \exp(-E_a/RT)$$

and Eyring:

$$k = kT/h \cdot \exp(dS/R - dH/RT) = kT/h \cdot \exp(-dG/RT).$$

The values for $t$, $dH$, $dS$ and $dG$ are given for 20°C. The rate constants of the mutant proteins were corrected for the effective surface proton concentration ($10^{-4.2}$ M; see Fig. 5).

| BR type | ($E_a$) (kJ/mol) | $f$ (1/s) | $t$ (ms) | $dH$ (kJ/mol) | $dS$ (J/mol·K) | $dG$ (kJ/mol) |
|---|---|---|---|---|---|---|
| BR | 75 (±5) | $2.5 (\pm 2) \cdot 10^{16}$ | 6 | 72.6 (±5) | +65 (±10) | 55 (±7) |
| D96 → G | 18 (±5) | $5.1 (\pm 5) \cdot 10^{7}$ | 200 | 15.6 (±5) | −106 (±10) | 47 (±7) |
| D96 → N | 32 (±5) | $1.3 (\pm 1) \cdot 10^{5}$ | 2430 | 29.6 (±5) | −60 (±10) | 47 (±7) |

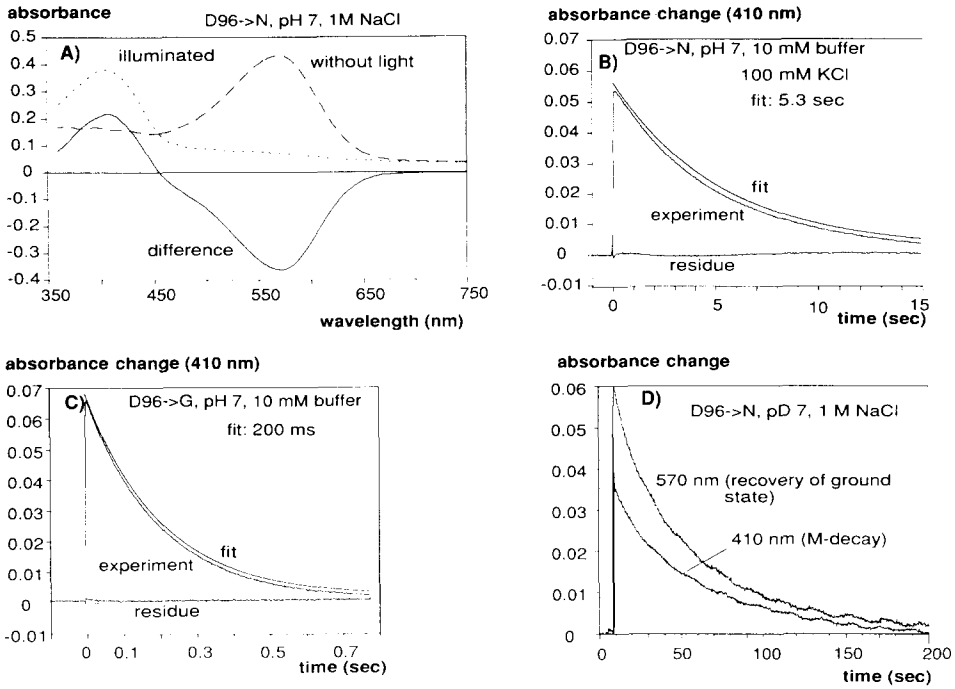


Fig. 1. Spectral and kinetic characteristics of point-mutated bacteriorodopsins. (A) absolute and different spectra of BR D96 → N in dark and light. (B) Decay of the M-intermediate of BR D96 → N fitted with a single exponential. The residue (experimental minus fit curve) demonstrates the monophasic nature of the reaction. (C) as B but mutant D96 → G. (D) M-decay (410 nm) and BR regeneration (570 nm) in mutant D96 → N. The 570 nm trace was inverted in sign for better comparison of the two processes.

retinylidene chromophore. The reaction followed first-order kinetics for both mutants (Fig. 1B and C) under all conditions applied, except for conditions causing very long lifetimes of M, in the range of 50–100 $s^{-1}$ (Fig. 1D). Concomitant with M-decay the absorption of the initial state of BR reappeared (Fig. 1D).

The lack of aspartic acid 96 as an internal proton donor in the BR molecule could cause an elevated free activation energy barrier for the reprotonation of the Schiff base, i.e., the M-decay. Table I summarizes the values found for the activation parameters of the reaction. Surprisingly, the Arrhenius energy of activation in the D96 → N mutant protein is only 32 kJ/mol as compared to 75 kJ/mol of the wild type, and the D96 → G mutant has an even lower value of 18 kJ/mol. Correspondingly, the pre-exponential factors of the reaction are dramatically small, causing a drastically enhanced contribution of the entropy of activation. Thus, according to the Eyring equation, the slow rate of reprotonation in the mutant proteins is caused by entropic rather than free energy factors of proton transfer. This reflects a situation where proton transfer to a group inside the protein (the C=N double bond), has to occur through a more random diffusive pathway than through a localized proton donor, which is a protonated amino-acid side-chain in the wild-type protein (D96). The activation energy for the pathway in the D96 → G mutant is 18 kJ/mol and comes close but does not reach the upper limit of 13 kJ/mol for diffusion-controlled proton transfer reactions in water [28]. Thus, the proton apparently diffuses also in the mutated protein with the help of amino-acid side-chains and water molecules as donors and acceptors which are separated by energy/entropy barriers. The placing of the protonated carboxylic acid group somewhere along the proton pathway in the wild-type protein causes not only optimization of speed but also renders the proton pump independent of external pH in the physiological range as described below.

*pH-dependence, isotope effects and influence of salt*

Fig. 2 shows the M-decay times as function of pH/p*D* in water and $D_2O$ for wild-type BR and the mutant proteins D96 → N and D96 → G. While no significant change in rate occurs in the range pH 4 to 8 for wild-type BR in water (see also Table II), a slight increase with p*D* is seen in $D_2O$. Both mutant proteins show in this pH/p*D* range a strong pH/p*D*-dependence of the M-decay rate. The logarithm of the inverse rate is plotted versus pH/p*D* in Fig. 2 and a slope of 1 would be expected for a bimolecular reaction of the proton with the Schiff base. Instead, a value of about 0.5 for the mutant was found, in agreement with similar measurements yielding values of 0.3 and 0.6 [13,14]. Although slight differences might be explainable by different experimental conditions none of the values comes close to 1. Differences in proton activity in the bulk phase and at the membrane surface would only

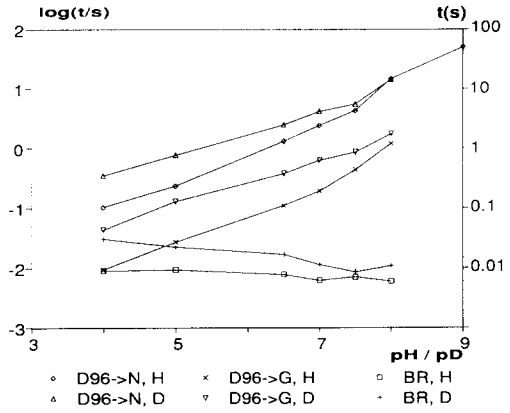


Fig. 2. Dependence of the M-decay in BR and the mutant proteins D96 → N and D96 → G on pH and p*D*. The decay time *t* (inverse of the rate constant) in seconds is plotted vs. pH/p*D*. Experiments were done at constant ionic strength of 10 mM buffer.

shift the curves on the abscissa but would not cause changes of the slope. We conclude therefore that an increase in proton activity of the bulk is not reflected by a proportional increase in that phase which is the actual proton reservoir for the transfer reaction (see Discussion).

The isotope effects of wild-type and both mutant proteins are summarized in Table III. The general tendency is a decrease of the isotope effect with increasing pH. For the wild-type and mutant D96 → N it drops from 3.4 at pH 4 to almost 1 at pH 8. The isotope effect is higher for mutant D96 → G and drops from 4.6 to 1.4 in the same pH interval. While none of the proteins comes close to theoretically possible values of the kinetic isotope effect [19], all three proteins apparently are different in the details of the mechanism of Schiff base reprotonation. In conclusion, we assume three different rate-limiting steps for the reprotonation reactions in the three bacteriorhodopsin structures (see Discussion).

The pH dependence of the reprotonation reaction in the mutant proteins predicts ionic strength dependent rates since BR in the purple membrane (together with

TABLE III

*Kinetic isotope effects on M-decay in BR and the mutant proteins D96 → N and D96 → G*

| [Ion] (mM) | pH | | | | | |
|---|---|---|---|---|---|---|
| | 4 | 5 | 6.5 | 7 | 7.5 | 8 |
| BR | | | | | | |
| 0.1 | | | | 2.0 | | |
| 1.0 | | | | 1.8 | | |
| 10.0 | 3.4 | 2.4 | 2.2 | 1.8 | 1.2 | 1.8 |
| 100.0 | | | | 1.8 | | |
| 1000.0 | | | | 1.3 | | |
| D96 → N | | | | | | |
| 0.1 | | | | 2.8 | | |
| 1.0 | | | | 2.1 | | |
| 10.0 | 3.4 | 3.3 | 1.9 | 1.7 | 1.3 | 1.0 |
| 100.0 | | | | 1.7 | | 1.1 |
| 1000.0 | | | 1.1 | 1.1 | 0.9 | 1.1 |
| D96 → G | | | | | | |
| 0.1 | | | | 4.6 | | |
| 1.0 | | | | 4.2 | | |
| 10.0 | 4.6 | 4.7 | 3.4 | 3.3 | 2.0 | 1.4 |
| 100.0 | | | | 3.3 | | 0.8 |
| 1000.0 | | | 2.7 | 1.4 | 2.7 | 1.5 |

TABLE II

*M-decay times (t in ms) in BR and mutant proteins at various pH (pD) values and ionic strength at 20°C*

| [Ion] (mM) | pH/p*D* | | | | | | | | | | | | |
|---|---|---|---|---|---|---|---|---|---|---|---|---|---|
| | 4 | | 5 | | 6.5 | | 7 | | 7.5 | | 8 | | 9 |
| | H | D | H | D | H | D | H | D | H | D | H | D | H |
| BR | | | | | | | | | | | | | |
| 0.1 | | | | | | | 8 | 16 | | | | | |
| 1.0 | | | | | | | 8 | 14 | | | | | |
| 10.0 | 9 | 31 | 9 | 23 | 8 | 17 | 6 | 12 | 7 | 9 | 6 | 11 | |
| 100.0 | | | | | | | 4 | 8 | | | | | |
| 1000.0 | | | | | | | 6 | 8 | | | | | |
| D96 → N | | | | | | | | | | | | | |
| 0.1 | | | | | | | 1090 | 3030 | | | | | |
| 1.0 | | | | | | | 1389 | 2933 | | | | | |
| 10.0 | 104 | 352 | 237 | 781 | 1332 | 2483 | 2427 | 4184 | 4290 | 5560 | 14700 | 14490 | 51020 |
| 100.0 | | | | | | | 4566 | 7575 | | | 26240 | 28400 | 99000 |
| 1000.0 | | | | | 5236 | 5600 | 13793 | 15650 | 25000 | 23000 | 55820 | 63290 | 163000 |
| D96 → G | | | | | | | | | | | | | |
| 0.1 | | | | | | | 113 | 518 | | | | | |
| 1.0 | | | | | | | 137 | 581 | | | | | |
| 10.0 | 10 | 44 | 27 | 129 | 111 | 382 | 195 | 636 | 440 | 870 | 1210 | 1750 | |
| 100.0 | | | | | | | 319 | 1037 | | | 2415 | 1940 | |
| 1000.0 | | | | | 433 | 1155 | 1170 | 1590 | 3570 | 9800 | 8330 | 12100 | |

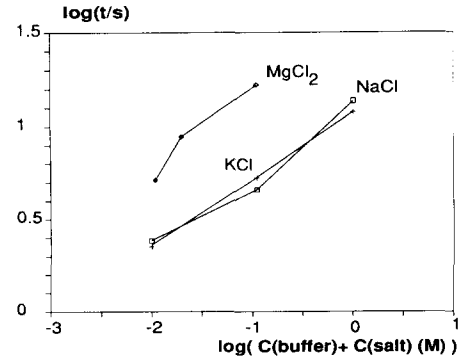


Fig. 3. Influence of different salts on M-decay kinetics in BR D96 → N. The decay time $t$ (inverse of the rate constant) in seconds is plotted logarithmically versus the logarithm of salt concentration (10 mM buffer plus varying salt concentrations).

lipids) forms an assembly of surface charges. The actual net charge at a given bulk pH and ionic strength will determine the local proton concentration responsible for the rate of proton transfer. In turn, pH and ionic strength will influence the net surface charge and thereby the rate. The expectation that increasing ionic strength causes increasing M-decay times is demonstrated by the experimental results shown in Figs. 3 and 4 and Table II, which document ionic strength effects for various conditions. From salt concentrations of 0.1 mM to 1 M wild-type BR has a constant rate of M-decay in water and changes its rate by a factor of 2 in $D_2O$ under the same conditions (Table II, upper panel). In contrast, both mutant proteins (pH 7) show changes of their M-decay rates of 10 (D96 → G) and 12.7 (D96 → N) in water and 3 and 5.1 in $D_2O$, respectively (Fig. 4 and Table II, lower panel). The ionic species influences the decay rate only by its charge, not by its chemical nature (Fig. 3). Finally, slowing the rate by increasing salt concentration also reduces the isotope effect (Table III). Thus, increasing ionic strength and decreasing proton concentration in the bulk cause the same kinetic phenomenon (for interpretation see Discussion).

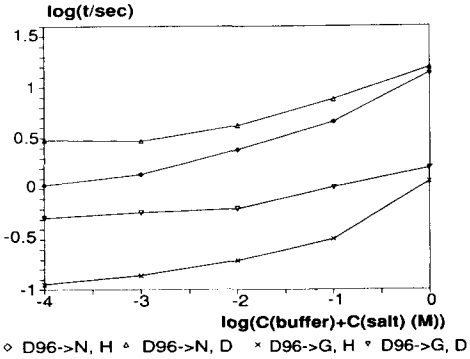


Fig. 4. Dependence of the M-decay in mutant proteins D96 → N and D96 → G on ionic strength (sodium chloride) in $H_2O$ and $D_2O$ at pH (p$D$) 7.

Summarizing our results, the removal of aspartic acid 96 renders the proton pump of bacteriorhodopsin dependent upon external pH and ionic strength. By variation of the experimental conditions the rate-limiting step of M-decay varies between a wild-type rate of about 10 ms and 3 min. The protonated carboxylic acid group at position 96 in the wild-type protein, on the other hand, serves two functions. It is responsible for the pH-independence of the proton pump, and due to its spatial localization in the protein structure it lowers the entropy of activation in the rate-limiting proton transfer reaction optimizing the turnover number of the pump.

## Discussion

Before a detailed interpretation of the mutational effects in BR is given, the introduction of a simplified scheme of proton transfer from the cytoplasm to the outer medium is appropriate. It is assumed that proton transfer occurs through the intrahelical pore of bacteriorhodopsin formed by its seven amphipathic helices. The wall of this pore should consist of relatively hydrophilic amino-acid side-chains, and the actual proton pathway may be formed by many of those residues, but also could include some water molecules (Dencher, N., personal communication). It is not known whether a defined path exists in which a proton can only hop from one place to the next or whether alternative proton-binding sites exist and thus many kinetically equal paths form a network of proton transfer steps. Two facts, however, should be kept in mind. The C=N double bond to and from which protons are transferred is not on the surface but about 17 A inside the protein [20]. Thus, the intrahelical pore is separated into two half pores or half channels. According to current models of the transmembrane folding of BR [30], aspartic acid 96 should be located on the half channel connecting the cytoplasm with the C=N double bond and is characterized by two very important properties. It is protonated up to pH values of 9, indicating that in the initial state $BR_{570}$ it is not equilibrating with the bulk pH, but becomes deprotonated only when the M-state decays [12] and, logically, it must receive a proton then from the bulk phase, indicating a conformational change allowing diffusional exchange with the surface not seen in $BR_{570}$. Alternatively, accessibility of apspartic acid 96 for protons exists also in $BR_{570}$, but the immediate environment drastically elevates the p$K$ of apartic acid 96.

A plausible model of the sequence of reactions in the catalytic cycle therefore assumes that in the M-state with a 13-*cis* retinylidene moiety proton transfer from aspartic acid 96 leads to the N-intermediate with the protonated Schiff base in the *cis* configuration, followed by isomerization to the *trans* state which might

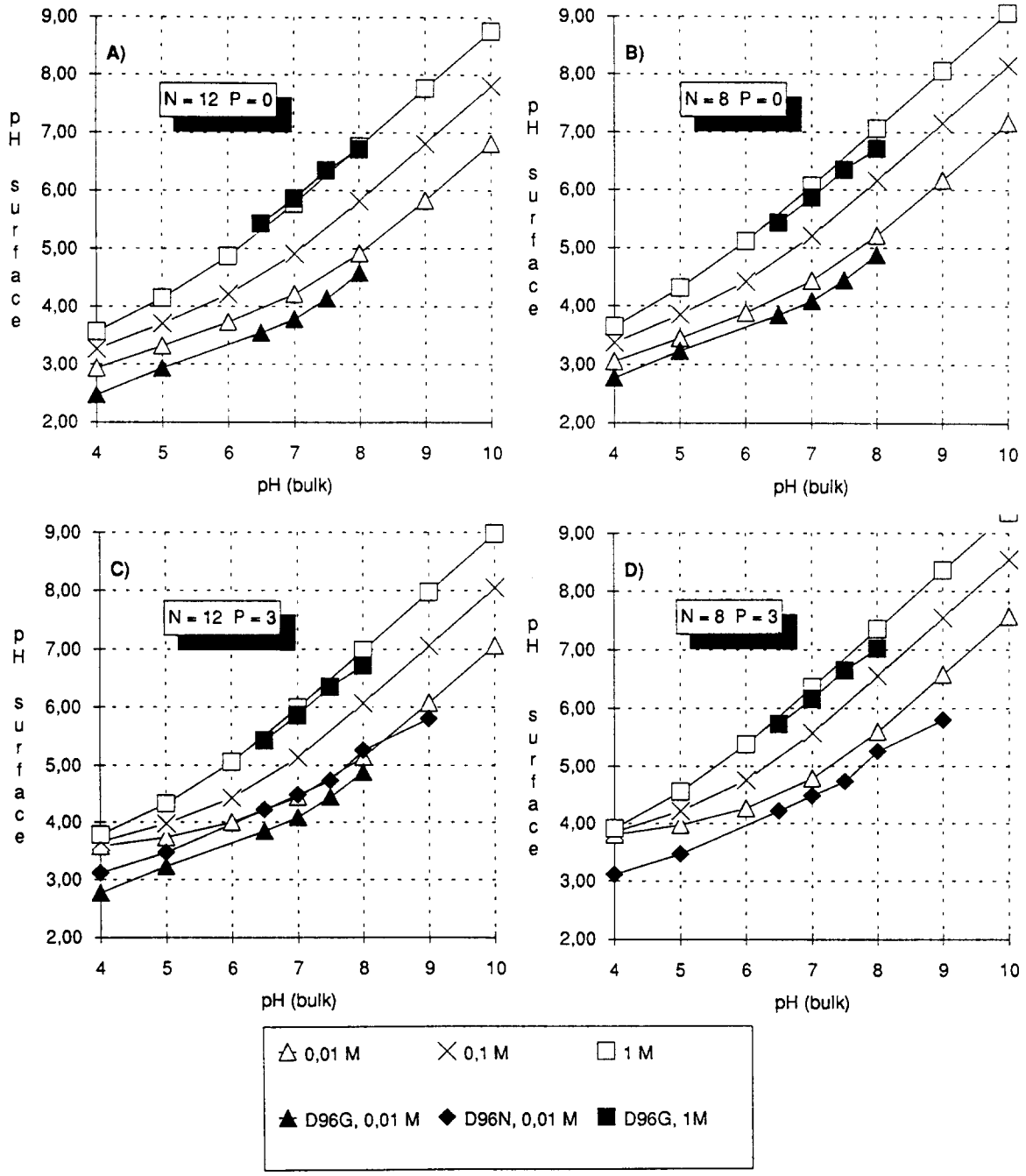


Fig. 5. Calculated surface pH values as a function of bulk pH for varying ionic strength and surface charge values $N$ and $P$ (empty symbols). $N$ are the negative charges with an assumed p$K$ 4, and $P$ are the positive charges with p$K > 10$. Calculations were done on the basis of Eqns. 1 to 4. Experimental values (filled symbols) were derived from the decay times and resulting curves are shifted arbitrarily on the ordinate to allow a better comparison of the slope of the curves.

be the *O*-intermediate. Connected to this isomerization could be the opening of the half channel for protonation of aspartic acid 96 with protons from the bulk phase. The isotope effect in the wild-type protein shows that protonation during M-decay apparently limits the rate, i.e., the protonated aspartic acid 96 donates a proton to the Schiff base faster than a deuterated aspartic acid 96. The limitation of the photocycle by the M to N transition is in accordance with a new recently published scheme of the photocycle in bacteriorhodopsin [21]. The proton transfer between water, aspartic acid 96 and C=N should not be considered as single step reactions, but an unknown number of intermediate proton accepting/donating groups can be involved. The replacement of aspartic acid 96 by asparagine removes one essential proton donor in the half channel and a different group, $x$, must be involved in the rate-limiting proton-transfer step of this mutant

protein because again a different isotope effect is found. Replacement of aspartic acid 96 by glycine apparently involves a third group, $y$, in the same channel, which shows the highest isotope effect of the three proteins. Thus, all three reprotonation pathways of the C=N double bond should be different and this is reflected clearly by the activation parameters being different for all three proteins. The Arrhenius activation energy of 18 kJ/mol in the glycine mutant is the lowest and might explain why this protein shows the largest isotope effect. More importantly, the results demonstrate that in none of the proteins does free diffusion of the proton, similar to that in a water phase, occur [22]. Instead, a set of groups must participate in either a chain-like or a network-like array of proton donors and acceptors with thermal barriers between them. The effect of the creation of an internal proton donor close to the Schiff base is seen mainly as the positive entropy change during the rate limiting proton-transfer step which drastically enhances the rate compared to the mutant proteins. This nicely demonstrates the kinetic optimization of the proton-transfer reaction producing an efficient proton pump. It should be mentioned that azide is able to mimic D96 kinetically in mutated proteins and might do so by physically being bound close or at the position of aspartic acid 96 [14].

In the mutant proteins, water, or a group exchanging protons with water, is the reaction partner of the retinylidene moiety. Apparently, delocalization of the reacting proton is reflected by the drastic delay of proton-transfer. At the same time external parameters, i.e., those of the bulk phase determine the rate.

The ionic strength dependence of reprotonation in the mutant proteins can be best explained on the basis of electrostatic potentials formed at the membrane-solution interfaces (for review see Ref. 23). The potential is influenced by ionic strength of the bulk and, in turn, influences the surface pH in the way outlined here. Consider a membrane with a net negative charge densitiy, $\sigma$, suspended in a medium of $z$-valent cations and anions. Anions will be repelled from and cations will be attracted to the membrane's surface according to electrostatic forces, but according to entropic forces all ions should be distributed homogeneously in the solution. The combination of the Poisson and Boltzmann equations then describes the surface potential $V_0$ as a function of surface charge density $\sigma$, ion valency $z$ and ion concentration $c_{ion}$ (Gouy-Chapman equation):

$$V_0(\sigma, z, C_{ion}) = \frac{2kT}{z \cdot e} \operatorname{arcsinh} \frac{\sigma}{\sqrt{8N_a C_{ion} \epsilon \cdot \epsilon_0 kT}} \quad (1)$$

$k$ is the Boltzmann constant, $T$ the absolute temperature, $e$ the elementary charge, $N_a$ Avogadro's number and $\epsilon$ and $\epsilon_0$ the dielectric constants of the medium and the vacuum, respectively.

The potential as function of distance from the surface is given as:

$$V(x) = V_0 \, e^{-\chi \cdot x} \text{ with } \chi = \sqrt{\frac{2e^2 \cdot N_a C_{ion} \cdot z^2}{\epsilon \cdot \epsilon_0 kT}} \quad (2)$$

Protons as cationic species accumulate at the negatively charged purple membrane's surface changing the pH at the surface according to:

$$pH_{interface} = pH_{bulk} + \frac{eV_0}{kT} \cdot 04343 \quad (3)$$

Eqns. 1 and 3 allow the calculation of the effective proton concentration at the interface as a function of bulk pH, ion valency, concentration of the ion in the medium and the surface charge of the membrane. One more complication occurs: The plot of log $t$ (time by which M concentration dropped to $1/e$ of its initial value) versus pH deviates from a straight line with a slope of 1, as would be expected for a standard bimolecular reaction between protons and the Schiff base. To explain this, two alternatives exist. Obviously, in the mutant protein another amino-acid side-chain could replace aspartic acid 96 as an internal proton donor. Accessibility for protons from outside must exist because otherwise no dependence on pH would be expected. Therefore a pH-dependence reflecting the p$K$ of that group would be expected. This, however, is not the case between pH 4 and 8. The alternative explanation for the broken reaction order with respect to protons is found by an extension of the surface charge consideration described above. The surface charge a in itself is pH-dependent if the groups involved have p$K$ values within the pH range considered [27].

$$\sigma = \frac{e}{F}\left(P - \frac{N}{1+10^{pK-pH}}\right) \cdot \exp\left(-\frac{eV_0}{kT}\right) \quad (4)$$

$N$ is the number of dissociable acid groups per bacteriorhodopsin molecule on its cytoplasmic surface with a p$K$ assumed here to be 4 and $F$ is the area per bacteriorhodopsin molecule (8.4 nm$^2$). In addition, $P$, the number of positively charged groups on the surface, influences $\sigma$ and was included in calculations which simulate the experimental findings. Fig. 6 shows selected results of these calculations with variations of $N$, $P$ and ionic strength but with a constant p$K$ of 4 for surface-located dissociable groups. As seen from Fig. 6A, our results at 10 mM ionic strength are best simulated with $N = 8$, $P = 0$ for the D96 → N mutant protein in the pH range of 4–8. (This $N$ value corresponds well with a surface charge density reported in Refs. 24, 25 and 29.)

Data from the literature [13] could be simulated with the same $N$ and $P$ value for the ionic strength of 150 mM applied in this work. Increasing the ionic strength

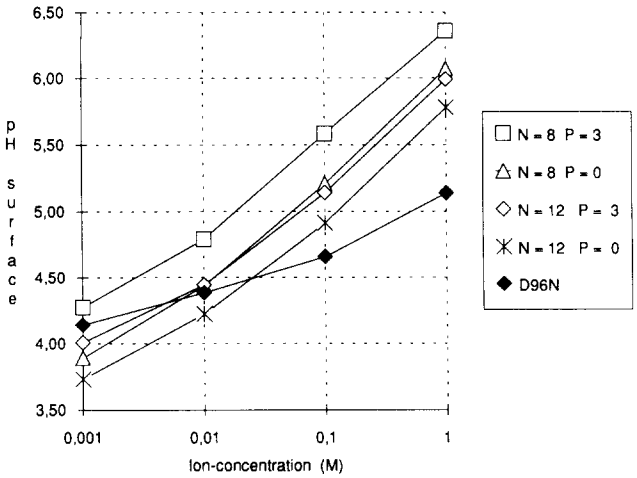


Fig. 6. *Calc*ulated surface pH as function of ionic strength in the bulk phase at constant pH of 7. Surface charges (N and P) were varied as indicated. One set of experimental values (filled symbols) was calculated as for Fig. 6 and is also shifted arbitrarily on the ordinate. For the different slope of experimental and theoretical curves see text.

to 1 M produces a slope of log $t$ vs. pH of 0.9 in the range of pH 7–9 and was found in our experiments (Table II and Fig. 5).

It is worthwhile mentioning that a slope of 1 was found for the reprotonation of the HR410 state in halorhodopsin when measured in 1 M salt and in the presence of azide [26]. In contrast, azide in mutant bacteriorhodopsin D96 → N eliminates pH-dependence, indicating a true replacement of D96 by azide as an internal proton donor (see above).

As demonstrated in Fig. 5, additional positive charges ($P = 3$, compare A and C) cause a decrease of slope in the low pH-range. A similar effect is seen for increasing $N$ values (B and A). A change in p$K$ would result in a shift of the curves on the $x$-axis without a change in shape (not shown). Increasing ionic strength causes the same effect as increasing the $P$ and $N$ values, but at high pH values the curves always approach a slope of 1.

It should be stressed that $N$ and $P$ do not indicate the number of dissociable groups actually present on the surface. Neither is the surface expected to be covered equally densely with charged groups, nor would groups equally contribute to the described influence on the proton-transfer rate because of the limited area of the pore's mouth where the protons enter. Charged lipids were also not considered. This might serve as an explanation why the dependence of surface pH on ionic concentration under various assumption of $N$ and $P$ values is not quantitatively reflected by the ionic strength dependence of the M-decay rate in the mutant proteins (Fig. 6). Nevertheless, the simulations demonstrate that surface charge effects can explain all phenomena observed in the mutant proteins.

## Acknowledgements

We thank S. Meessen for preparation of purple membranes and J. Tittor for critical reading of the manuscript.

## References

1 Lipscomb, W.N. (1971) Proc. Robert A. Welch Found. Conf. Chem. Res. 15, 150.
2 Fersht, A. (1985) in Enzyme Structure and Mechanism, W.H. Freeman & Co., Reading.
3 Roepe, P.D., and Kaback, H.R. (1989) Proc. Natl. Acad. Sci. USA 86, 6087–6091.
4 Overath, P. and Wright, J.K. (1983) Trends Biochem. Sci. 8, 404–408.
5 Althoff, G., Lill, H. and Junge, W. (1989) J. Membr. Biol. 108, 263–271.
6 Oesterhelt, D. (1976) Angew. Chem. Int. Edn. 15, 17/24.
7 Michel, H., Epp, O. and Deisenhofer, J. (1986) EMBO J. 5, 2445–2451.
8 Oesterhelt, D. and Tittor, J. (1989) Trends Biochem. Sci. 14, 57–61.
9 Dencher, N., Burghaus, P. and Gresziek, S. (1986) Methods Enzymol. 127, 746–760.
10 Hess, B. and Oesterhelt, D. (1973) Eur. J. Biochem. 37, 316–326.
11 Butt, H.J., Fendler, K., Bamberg, E., Tittor, J. and Oesterhelt, D. (1989) EMBO J. 8, 1657–1663.
12 Gerwert, K., Hess, B., Soppa, J. and Oesterhelt, D. (1989) Proc. Natl. Acad. Sci. USA 86, 4943–4947.
13 Holz, M., Drachev, L.A., Mogi, T., Otto, H., Kaulen, A.D., Heyn, M., Skulachev, V.P. and Khorana, H.G. (1989) Proc. Natl. Acad. Sci. USA 86, 2167–2171.
14 Tittor, J., Soell, C., Oesterhelt, D., Butt H.-J. and Bamberg, E. (1989) EMBO J. 8, 3477–3482.
15 Oesterhelt, D. and Krippahl, G. (1983) Ann. Microbiol. (Inst. Pasteur) 134B 137–150.
16 Soppa, J. and Oesterhelt, D. (1989) J. Biol. Chem. 264, 13043–13048.
17 Soppa, J., Otomo, J., Straub, J., Tittor, J., Messen, S. and Oesterhelt, D. (1989) J. Biol. Chem. 264, 13049–13056.
18 Covington, A.K., Paabo, M., Robinson, R.A. and Bates, R.G. (1968) Anal. Chem. 40, 700–706.
19 Bell, R.P. (1974) Chem. Soc. Rev. 3, 513–544.
20 Hauss, T., Otto, H., Grzesiek, Westerhausen, J. and Heyn, M.P. (1989) Biophys. J. 55, 254a.
21 Chernavskii, D.S., Chizhov, I.V., Lozier, R.H., Murina, T.M., Prokhorov, A.M. and Zubov, B.V. (1989) Photochem. Photobiol. 49, 649–653.
22 Renthal, R. (1981) J. Biol. Chem. 256, 11471–11476.
23 McLaughlin, S. (1977) Curr. Topics Membr. Transp. 9, 71–144.
24 Kuschmitz D. and Hess, B. (1981) Biochemistry 20, 5950–5957.
25 Renthal, R. and Cha, C.-H. (1984) Biophys. J. 45, 1001–1006.
26 Hegemann, P., Oesterhelt, D. and Steiner, M. (1985) EMBO J. 4, 2347–2350.
27 Miller, A., Helm, C.A. and Moehwald, H. (1987) J.Phys. 48, 693–701.
28 Eigen, M. and DeMaeyer, L. (1955) Z. Elektrochem. 59, 986–993.
29 Szundi, I. and Stoeckenius, W. (1989) Biophys. J. 56, 369–383.
30 Henderson, R., Baldwin, J.M., Ceska, T.A., Zemlin, F., Beckmann, E. and Downing, K.H. (1990) J. Mol. Biol. 213, 899–929.